Talanta 88 (2012) 524–532

Contents lists available at SciVerse ScienceDirect

Talanta

journal homepage: www.elsevier.com/locate/talanta

# Combined voltammetric and spectroscopic analysis of small molecule–biopolymer interactions: The levodopa and serum albumin system

Qiulan Zhang [a], Yongnian Ni [a,b,*], Serge Kokot [c]

[a] State Key Laboratory of Food Science and Technology, Nanchang University, Nanchang 330047, China
[b] Department of Chemistry, Nanchang University, Nanchang 330031, China
[c] Chemistry, Faculty of Science and Technology, Queensland University of Technology, Brisbane 4001, Australia

ARTICLE INFO

*Article history:*
Received 13 August 2011
Received in revised form 31 October 2011
Accepted 3 November 2011
Available online 15 November 2011

*Keywords:*
Levodopa
Bovine serum albumin
Fluorescence
Voltammetry
Multivariate curve resolution–alternating least squares

ABSTRACT

An analytical method was researched for the simultaneous determination of reactants and products during the binding of important small molecules such as levodopa (LD) with biopolymers such as bovine serum albumin (BSA). Voltammetry and fluorescence spectroscopy were used to obtain the analytical profiles from different reactant mixtures as a function of concentration. This enabled the extraction of the equilibrium constants ($K_{SV}$) which are reported for the first time. Voltammetric results supported the formation of the LD–BSA complex but not that with dopamine. Further information of the LD–BSA system was unattainable because the measured composite profiles could not be extracted.

New information was obtained when the extended data matrix was resolved by the MCR–ALS method. The previously unavailable extracted voltammogram profile of LD–BSA complex indicated that the complex was electroactive; this was unexpected if the LD–BSA system was in its folded state, and hence, it was suggested that the protein must be unfolded. The observation that the drug:BSA stoichiometry was 3:1, i.e. $(levodopa)_3$–BSA, supported this suggestion; these results were obtained from the MCR–ALS extracted concentration profiles for the three reaction components.



## 1. Introduction

In general, there are many examples of complex reactions for which it is not only important to analyse the reactants but also the products. However, it can be quite difficult to analyse a multi-component reaction system, especially if one or more of the reaction species are complex. Typical illustrations of such systems are the interactions of small molecules with DNA or proteins, and it is often desirable to estimate simultaneously, the amounts of the small molecule, the biopolymer and their complex product. Such analytical tasks can be quite challenging, and composite profiles of the reactants and products are collected from instrumental analyses. Thus, the application of the common methods of data interpretation is often limited. However, chemometrics methods such as multivariate curve resolution–alternating least squares (MCR–ALS) [1], have provided a potential solution to resolve the analytical profile complexities.

It is also possible, with the use of the expanded matrix methods [2], to combine data matrices of analyte profiles derived from different analytical methods, which are commonly based on the same or similar techniques e.g. HPLC–DAD measurements at two different wavelengths [3]. In general, the results of such approaches have indicated that the increased information in the expanded matrix improves data analysis and subsequent interpretation of the results. However, combination of data matrices derived from very different analytical techniques e.g. voltammetry and some form of spectroscopy or chromatography, which monitor different properties of the analytes in the system, are much less common. It is this area of analysis, which is explored in the present investigation with the use of voltammetry and fluorescence spectroscopy for the analyses of a drug molecule, levodopa, in the presence of bovine serum albumin (BSA) and their complex product.

Levodopa (LD, 3-(3,4-dihydroxyphenyl)-L-alanine), is the preferred drug for the treatment of the debilitating, well-known Parkinson's disease, which is caused by a deficiency of the neurotransmitter, dopamine, in the brain [4]. This deficiency cannot be readily made-up by oral administration of this drug because it cannot penetrate the blood–brain barrier (BBB). However, LD can cross this barrier and then be metabolized to dopamine, thus reducing the deficiency [5]. Unfavorable physicochemical properties hinder the transport of several entities across the BBB and thereby limit their utility as central nervous system (CNS) – active agents. The micro-vessel endothelium in the brain is a barrier for the passive transport of hydrophilic substances into that organ [6]. Such

* Corresponding author at: Department of Chemistry, Nanchang University, Nanchang 330031, China. Tel.: +86 791 3969500; fax: +86 791 3969500.
*E-mail addresses:* ynni@ncu.edu.cn (Y. Ni), s.kokot@qut.edu.au (S. Kokot).

0039-9140/$ – see front matter © 2011 Elsevier B.V. All rights reserved.
doi:10.1016/j.talanta.2011.11.027

obstacles to the CNS penetration of therapeutic agents have been in the past circumvented by approaches that rely on the synergy of more than one disciplines; e.g. chemistry-based (lipophilic drugs), biology-based approaches (carrier/receptor mediated transport) and drug delivery based (intrathecal/interstitial/olfactory – delivery) [7]. An approach that encompassed covalent linkage of the drug to a carrier that can be recognized by a specific transport protein and hence, be transported, has found some interest in recent years.

Serum albumin (SA) is the most abundant protein in plasma, and participates in the binding and transportation of various ligands such as fatty acids, hormones, and drugs. The distribution, free concentration, and metabolism of these ligands strongly depend on their thermodynamic parameters and binding constants with SA [8]. BSA is a well known protein, particularly because it is structurally similar to the human serum albumin (HSA). It is a small protein with a single polypeptide chain, which is cross-linked by 17 disulfide bonds [9]. In the presence of small ligands, BSA often forms complexes, which apparently participate in the ligand–cell interactions at cell surfaces [10]. However, on the whole, little is known about the molecular mechanism by which the interaction takes place and also about the role that LD–SA complexes play in the uptake of the drug by the cell.

In general, the common methods used to investigate the interaction of proteins with small molecules include: UV–vis spectrophotometry [11], FT-IR [12], electrochemistry [13], capillary electrophoresis [14], HPLC [15], and NMR [16] among others; some of these methods have been used to investigate the interaction of small molecules with biopolymers with the aid of chemometrics [17,18].

Vives et al. [2] investigated the interaction of some drugs with polynucleotides at equilibrium with the use of several spectroscopic techniques; they applied multivariate extension of the continuous variation and mole-ratio methods to obtain qualitative and quantitative information of the binding equilibrium. Subsequently, the spectral results were resolved with the use of MCR–ALS. Likewise, the interpretation of results from electrochemical methods of analysis is significantly improved with the use of powerful chemometrics tools, such as MCR–ALS. Gusmao et al. [19] and Chekmeneva et al. [20] applied the MCR–ALS method to data collected by different voltammetric techniques for the analysis of processes involving metal complexes. The use of chemometrics in electro-analytical chemistry is not as common as in spectroscopy, although as recently reviewed [21], the application of these methods in electro-analysis for mathematical resolution of overlapping signals, calibration and model identification has increased. Multidimensional instrumental signals can be readily collected with the use of ever improving modern instrumentation, and from this information, extension matrices may be constructed, which facilitate the quantitative analysis of increasingly complex samples [22]. Fluorescence spectroscopy can provide valuable qualitative and quantitative information about the binding of ligands to serum albumin, e.g. ligand–albumin interactions and the estimation of binding constants, respectively [23]. In general, electrochemical analysis is simple, easily implemented, low costing and fast; as well, electrochemical data can contribute to the elucidation of the interaction of drugs with biomolecules [24], but voltammetric methods are still less preferred for analysis. In this work, fluorescence and electrochemistry were applied for the study of the interaction of LD with BSA.

The objectives of this study were:

1. To research and develop analytical methodology so as to investigate the interaction of the important ligand, levodopa (and to a lesser extent dopamine), with the common transport protein, serum albumin, in the form of BSA.
2. To perform simultaneous analysis for the reactants mentioned above and their LD–BSA complex product as a function of concentration, and to carry out this analysis with the aid of three separate techniques, cyclic (CV) and linear sweep (LSV) voltammetry and fluorescence spectroscopy so as to obtain different information about the above interaction as well as the thermodynamic parameters involved.
3. To construct a combined data matrix from the fluorescence and voltammetric measurements by means of the expanded matrix approach, and then, to analyse this information with the use of the MCR–ALS chemometrics method so as to resolve the overlapping reactant/product profiles.
4. To interpret the concentration profiles derived from the analysis in #3 above so as to describe the progress of the interaction as a function of concentration, and to demonstrate the possibilities of extracting otherwise unavailable information with the use of this multi-dimensional approach.

## 2. Material and methods

### 2.1. Instrumentation

All fluorescence spectra were measured on a Perkin-Elmer LS-55 spectrofluorometer equipped with a thermostatic bath (Model ZC–10, Ningbo Tianheng Instruments Factory, China) and a 1.0 cm quartz cuvette. The excitation and emission slits were set at 10 nm, while the scanning rate was 1500 nm $min^{-1}$. The FL Winlab software (Perkin-Elmer) was used to correct the measured data.

Electrochemical measurements were carried out on a CHI-660A electrochemical workstation (Chenhua Instrumental Company, Shanghai). A glassy carbon working electrode (2 mm diameter) was used; it was polished with graded 10 μM alumina powder, and rinsed with doubly distilled water prior to application. A platinum wire auxiliary electrode and a commercial saturated Ag/AgCl reference electrode were included in the system. All measurements were carried out at room temperature ($25 \pm 0.5\,^{\circ}C$) unless stated otherwise.

### 2.2. Materials

A stock solution of $3 \times 10^{-3}$ mol $L^{-1}$ levodopa (Sigma; purity – not less than 99.0%) was prepared by dissolving its crystals (0.0302 g) in 50 mL hydrochloric acid (pH 4.0). BSA ($2 \times 10^{-3}$ mol $L^{-1}$) was prepared by dissolving 1.36 g of the purified protein ($M$ = 68,000 Da; Bomei Biological Co. Ltd., Hefei, China) in 10.0 mL $5.0 \times 10^{-2}$ mol $L^{-1}$ sodium chloride solution and stored at 4 °C. To confirm the purity of the prepared BSA ($2 \times 10^{-3}$ mol $L^{-1}$), the concentration was diluted to $1.47 \times 10^{-5}$ mol $L^{-1}$, and the measured absorbance value was 0.660 at 278 nm. Based on a reference absorbance value of 0.667 at 278 nm for 1.0 g $L^{-1}$ ($1.47 \times 10^{-5}$ mol $L^{-1}$) pure BSA [25], the purity of the prepared BSA was 99%. All experimental solutions were adjusted with the Tris–HCl ((hydroxy methyl) amino methane–hydrogen chloride) buffer to pH 7.4. Other chemicals were Analytical grade reagents, and doubly distilled water was used throughout.

### 2.3. Procedures

Solutions used in the fluorescence experiments were prepared in Tris–HCl buffer (3.0 mL; pH 7.4) containing appropriate amounts of BSA and levodopa. The total added volume (BSA and levodopa) was less than 0.1 mL. Titrations were performed manually using suitable micropipettes. A mixed solution was shaken thoroughly and equilibrated for 10 min at 298 K. Fluorescence spectra were then measured in the range of 200–550 nm at the maximum excitation wavelength of 280 nm.

Solutions used in the voltammetric experiments were prepared in Tris–HCl buffer (10.0 mL; pH 7.4) containing appropriate amounts of BSA and levodopa. The total added volume (BSA and levodopa) was less than 0.2 mL. A given levodopa–BSA system was stirred for 10 s, and then the sample was analysed as required, either by linear sweep voltammetry or cyclic voltammetry, over a scanning potential range of 0.1–1.0 V, and a scanning rate of 100 mV $s^{-1}$.

*2.3.1. Fluorescence quenching study*

The concentration of BSA was kept constant ($5.00 \times 10^{-8}$ mol $L^{-1}$) throughout, and levodopa or dopamine, as appropriate, was added to this solution in the range of 0.00–$6.67 \times 10^{-7}$ mol $L^{-1}$ (in steps of $8.33 \times 10^{-8}$ mol $L^{-1}$). The well-mixed solutions were allowed to stand for 10 min at 298, 301 and 304 K before spectroscopic measurements.

*2.3.2. Cyclic voltammetry (CV) of levodopa samples*

Concentration of levodopa was kept at $3.00 \times 10^{-5}$ mol $L^{-1}$ and the BSA solution was added at different concentrations in the range of 0.00–$8.00 \times 10^{-6}$ mol $L^{-1}$ (in steps of $1.00 \times 10^{-6}$ mol $L^{-1}$). Each given levodopa-BSA solution was stirred for 10 s and then the CV experiment was performed at pH 7.4.

*2.3.3. Development of the expanded data matrix for MCR–ALS*

*Experiment 1 (voltammetric method, $\boldsymbol{D}_{LSV}^{LD}$)*: The concentration of levodopa was kept constant ($3.00 \times 10^{-5}$ mol $L^{-1}$), and BSA was added to the solution in the range of 0.00–$1.80 \times 10^{-5}$ mol $L^{-1}$ (in steps of $1.00 \times 10^{-6}$ mol $L^{-1}$).

*Experiment 2 (fluorescence method, $\boldsymbol{D}_{F}^{LD}$)*: The concentration of levodopa was kept constant ($2.00 \times 10^{-7}$ mol $L^{-1}$), and BSA was added to the solution in the range of 0.00–$1.20 \times 10^{-7}$ mol $L^{-1}$ (in steps of $6.67 \times 10^{-9}$ mol $L^{-1}$).

*Experiment 3 (voltammetric method, $\boldsymbol{D}_{LSV}^{BSA}$)*: The concentration of BSA was kept constant ($1.00 \times 10^{-5}$ mol $L^{-1}$), and levodopa was added to the solution in the range of 0.00–$5.4 \times 10^{-5}$ mol $L^{-1}$ (in steps of $3.00 \times 10^{-6}$ mol $L^{-1}$).

*Experiment 4 (fluorescence method, $\boldsymbol{D}_{F}^{BSA}$)*: The concentration of BSA was kept constant ($6.67 \times 10^{-8}$ mol $L^{-1}$), and levodopa was added to the solution in the range of 0.00–$3.60 \times 10^{-7}$ mol $L^{-1}$ (in steps of $2.00 \times 10^{-8}$ mol $L^{-1}$).

For the LSV analysis, the scanning potential range was 0.10–1.00 V being sampled at every 0.01 V, and the fluorescence spectra were recorded over the 250–450.5 nm range being sampled at every 0.5 nm, respectively.

### 2.4. Chemometrics method: multivariate curve resolution–alternating least squares (MCR–ALS)

The goal of MCR is to decompose composite measured profiles such as spectra, voltammograms or chromatograms into the different pure profiles for each species in a mixture. The resulting extracted information for the pure components may be in the form of single bands or more complex profiles. Such data can be arranged into $\boldsymbol{D}$ ($M \times N$) matrix with $M$ objects and $N$ variables e.g. wavelength (nm) or potential (mV). The algorithm for MCR has been previously described in detail [26], and here only a working summary is provided. The MCR decomposition of a matrix is carried out according to the equation:

$$\boldsymbol{D} = \boldsymbol{C}\boldsymbol{S}^{T} + \boldsymbol{E} \quad (1)$$

where $\boldsymbol{D}$ is the matrix of the experimental data, with dimensions of $M \times N$. The matrix, $\boldsymbol{C}$ ($M \times F$), describes the individual contributions (concentration profiles) of the $F$ species involved in the given measured profiles. The matrix, $\boldsymbol{S}^{T}$ ($F \times N$), is then the contribution of the measured profiles of these $F$ species in the $N$ columns of the data matrix (pure measured profiles). $\boldsymbol{E}$ ($M \times N$) is the matrix of residuals, which contains the data variance unexplained by the product, $\boldsymbol{C}\boldsymbol{S}^{T}$.

One important and frequently used iterative approach to solve Eq. (1) is MCR by alternating least squares (ALS). The optimization process starts from initial guesses of $\boldsymbol{C}$ and $\boldsymbol{S}^{T}$, and these are then refined to yield profiles with chemical meaning.

When the same chemical system is monitored using more than one technique, e.g. fluorescence spectroscopy and LSV, a matrix is constructed, which consists of row-wise and column-wise augmented data, i.e. two types of information are presented. The individual data matrices corresponding to the two types of technique and the two different mole-ratio experiments are placed side-by-side. The related bilinear model for MCR–ALS analysis is shown below:

$$\begin{bmatrix} \boldsymbol{D}_{LSV}^{LD} & \boldsymbol{D}_{F}^{LD} \\ \boldsymbol{D}_{LSV}^{BSA} & \boldsymbol{D}_{F}^{BSA} \end{bmatrix} = \begin{bmatrix} \boldsymbol{C}^{LD} \\ \boldsymbol{C}^{BSA} \end{bmatrix} [\, \boldsymbol{S}_{LSV}^{T} \quad \boldsymbol{S}_{F}^{T} \,] + [\, \boldsymbol{E}_{LSV} \quad \boldsymbol{E}_{F} \,] \quad (2)$$

If $\boldsymbol{D}_F$ and $\boldsymbol{D}_{LSV}$ are the measurements for the two experiments obtained with the two techniques, there are two matrices of concentration profiles, $\boldsymbol{C}^{LD}$ and $\boldsymbol{C}^{BSA}$, valid for the two sets of raw measurements, and two row-wise augmented matrices of measured profiles, $\boldsymbol{S}_{F}^{T}$ and $\boldsymbol{S}_{LSV}^{T}$, which contain the pure profiles for the techniques used to obtain $\boldsymbol{D}_F$ and $\boldsymbol{D}_{LSV}$, respectively. Solving Eq. (2) for $\begin{bmatrix} \boldsymbol{C}^{LD} \\ \boldsymbol{C}^{BSA} \end{bmatrix}$ and $[\, \boldsymbol{S}_{F}^{T} \quad \boldsymbol{S}_{LSV}^{T} \,]$, facilitates the extraction of the related measured profiles of all the species in the system [26].

When the matrix $\begin{bmatrix} \boldsymbol{D}_{LSV}^{LD} & \boldsymbol{D}_{F}^{LD} \\ \boldsymbol{D}_{LSV}^{BSA} & \boldsymbol{D}_{F}^{BSA} \end{bmatrix}$ of the four data matrices is being built, the number of analyte species, $F$, can be obtained with the aid of EFA (Evolving Factor Analysis) [27] or PCA (Principal Component Analysis) or other methods based on factor analysis. The EFA method provides an estimation of the regions or windows where the concentration of different components is changing or evolving, and it also provides an initial estimation of how these concentration profiles change during the experiment. This method is based on the evaluation of the magnitude of the eigenvalues associated with all the submatrices of a matrix built up by adding successively all the rows of the original data matrix. The calculation is performed in two directions: forward (in the direction of the experiment) and backward (in the opposite direction of the experiment), e.g. Abdollahi and Mahdavi illustrate how concentration profiles obtained from EFA may be used as initial estimates for the concentration matrix input in the constrained ALS optimization [28]. PCA, an alternative approach to EFA, is a common chemometrics tool; it yields the number and direction of the relevant sources of variation in a bilinear data set [29]. Once the PCs, $F$, are determined and an initial estimate of their concentration profiles is obtained, it becomes easier to obtain improved estimates of either the concentration values or pure measured profiles. Constraints in ALS optimization, such as non-negative and unimodal solutions, are implemented to facilitate the finding of pure or most representative contributions to the data matrix using real variables. The resolution methods start with initial estimates of $C$ and work by optimizing iteratively the concentration, while introducing the available information about the system [29]. During the optimization, the above constraints are applied to ensure that the final solution is chemically meaningful [30].

However, the solutions to Eq. (1) obtained by MCR–ALS are not unique. They can have rotational and intensity ambiguities. To solve this limitation, column- and row-wise augmentation schemes (Eq. (2)) can be used for simultaneous resolution. This kind of simultaneous data analysis is more powerful compared to that described by Eq. (1) and allows for improved resolution of very complex

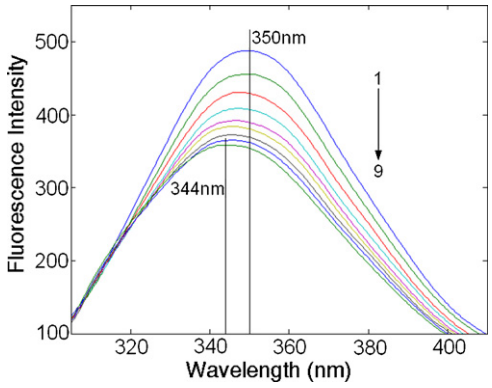


**Fig. 1.** Fluorescence emission spectra of the binary complex, levodopa–BSA.

data structures [26]. In general, this method should be useful to overcome some uncertainties in the analysis of the data related to coincidental processes or small signal shifts [31]. Thus, in this work, the data matrices, $\boldsymbol{D}_{\mathrm{LSV}}^{\mathrm{LD}}$ (experiment 1) and $\boldsymbol{D}_{F}^{\mathrm{LD}}$ (experiment 2), and $\boldsymbol{D}_{\mathrm{LSV}}^{\mathrm{BSA}}$ (experiment 3) and $\boldsymbol{D}_{F}^{\mathrm{BSA}}$ (experiment 4) were obtained, and an expanded data matrix, $\begin{bmatrix} \boldsymbol{D}_{\mathrm{LSV}}^{\mathrm{LD}} & \boldsymbol{D}_{F}^{\mathrm{LD}} \\ \boldsymbol{D}_{\mathrm{LSV}}^{\mathrm{BSA}} & \boldsymbol{D}_{F}^{\mathrm{BSA}} \end{bmatrix}$, was constructed by the combination of two row-wise and two column-wise data matrices. Subsequently, this was resolved by the MCR–ALS approach.

## 3. Results and discussion

### 3.1. Analysis of fluorescence quenching mechanism of BSA by levodopa and dopamine

BSA has two tryptophan (Trp) residues that possess intrinsic fluorescence: Trp-212, located within a hydrophobic binding pocket of the protein, and Trp-134, located on the surface of the molecule. Tryptophan emission dominates the BSA fluorescence spectrum in the UV region. When other molecules interact with BSA, tryptophan fluorescence may change depending on the impact of such interaction on the fluorophore–quencher complex [32]; this is often manifested in the decrease of the quantum yield of fluorescence from the fluorophore i.e. the BSA, and can be induced by a variety of molecular interactions with the quencher molecule. It has been suggested that when small molecules interact with BSA conformational changes occur in the protein's structure. This is attributed to changes in the intermolecular forces, which stabilize the secondary structure of the protein [33]. Thus, in this work, conformational changes of BSA were explored by measuring the intrinsic fluorescence intensity of BSA before and after addition of LD in Tris–HCl buffer (pH 7.40). In a separate similar experiment, dopamine replaced LD. On the addition of LD to BSA, the intensity of the main broad spectral emission band ($\lambda_{\max}$ = 350 nm) decreased gradually and shifted to about 344 nm (Fig. 1). This band shift was attributed to a change in the environment around the tryptophan residues as well as to an increase in hydrophobicity [34].

Fluorescence quenching refers to any process, which decreases the fluorescence intensity of a sample, and quenching mechanisms are usually classified as dynamic or static. They are distinguished by their different temperature and viscosity dependence; thus, dynamic quenching depends on diffusion, and therefore, the bio-molecular quenching constants are expected to increase with increasing temperature. In contrast, increased temperature is likely to result in lower values of the static quenching constants.

**Table 1**
Stern–Volmer quenching constants at different temperatures for the interaction of levodopa and dopamine with BSA.

| $T$ (K) | Levodopa $K_{\mathrm{SV}}$ ($\times 10^5$ L mol$^{-1}$) | $R^a$ | Dopamine $K_{\mathrm{SV}}$ ($\times 10^5$ L mol$^{-1}$) | $R^a$ |
|---|---|---|---|---|
| 298 | 5.80 | 0.998 | 4.63 | 0.999 |
| 301 | 5.25 | 0.998 | 4.93 | 0.998 |
| 304 | 4.67 | 0.998 | 5.30 | 0.997 |

[a] Linear correlation coefficient.

For fluorescence quenching, the decrease in intensity is usually described by the well-known Stern–Volmer equation [35]:

$$\frac{F_0}{F} = 1 + K_{\mathrm{SV}}[Q] \tag{3}$$

where $F_0$ and $F$ denote the steady-state fluorescence intensities in the absence and in the presence of the quencher. $K_{\mathrm{SV}}$ is the Stern–Volmer quenching constant, and [$Q$] is the concentration of the quencher. The degree of fluorescence quenching as a function of temperature when LD was added to BSA, was clearly discernable but moderate. The values of $K_{\mathrm{SV}}$ (Table 1) decreased with increase in temperature, which indicated that the probable quenching mechanism of this interaction was initiated by the formation of a complex rather than by dynamic collision.

Dopamine is the decaboxylated form of levodopamine and is the key molecule for reducing the symptoms of Parkinson's disease; hence, a similar temperature dependent experiment was performed with this substance (Illustrator 1).

The $K_{\mathrm{SV}}$ values measured at the same temperatures as above, for both the LD and dopamine interactions with the BSA, are reported for the first time, and are similar in magnitude ($\sim(4.00–6.00) \times 10^5$ L mol$^{-1}$). However, for dopamine, in contrast to LD, they increased with temperature (Table 1). This indicated that the probable quenching mechanism of the dopamine–BSA interaction was achieved via a dynamic collision rather than the formation of a complex, and thus, dopamine was unlikely to bind with the protein [36]. Dynamic quenching only affects the excited states of the fluorophores and no changes in the absorption spectra are expected. Structural changes due to complex formation may be investigated by UV–vis spectroscopy [37], and thus, UV–vis absorption spectra of BSA in the range of 200–400 nm collected in the absence and presence of dopamine should be quite similar if no significant drug-protein binding occurs. Spectra of BSA ($2.5 \times 10^{-6}$ mol L$^{-1}$), dopamine ($2.5 \times 10^{-6}$ mol L$^{-1}$), and their mixture ($2.5 \times 10^{-6}$ mol L$^{-1}$) in pH 7.4 buffer were collected; their difference spectrum i.e. spectrum (mixture dopamine/BSA–dopamine) should approximately resemble the spectrum (BSA). The observed result showed that the difference spectrum was actually quite similar to that of the BSA. This result supported the conclusions from the $K_{\mathrm{SV}}$ estimates above, and suggested a reason why dopamine cannot penetrate the BBB i.e. the common BSA–drug transport pathway is unavailable to it. Being the most delicate organ of the body, the brain is protected against potentially toxic substances by the BBB, which restricts the entry of most pharmaceuticals into the brain. The developmental process for new drugs for the treatment of CNS disorders has not kept pace with progress in molecular neurosciences because most of the new drugs discovered are unable to cross the BBB. The clinical failure of CNS drug delivery may be attributed largely to a lack of appropriate drug delivery systems [38]. LD, the standard for the treatment of Parkinson's disease, enters CNS via the large neutral amino acid transporters at BBB and is enzymatically cleaved in the brain to release dopamine [39].

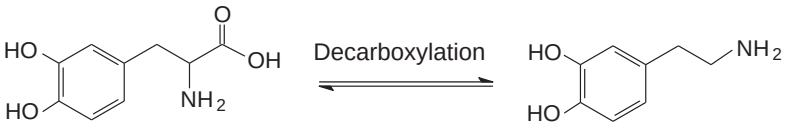


**Illustrator 1.**

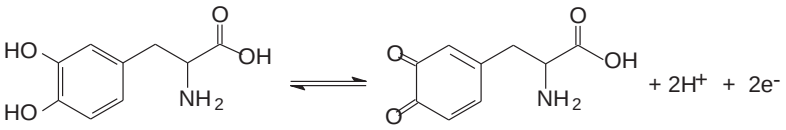


**Illustrator 2.**

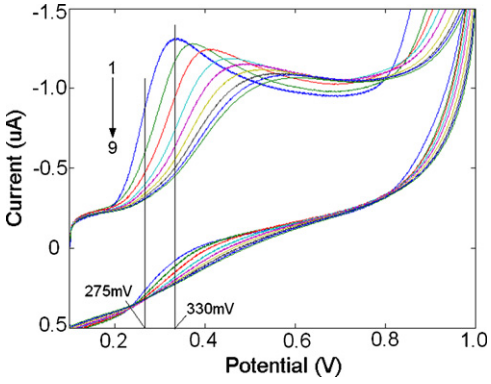


**Fig. 2.** Cyclic voltammograms of mixtures of levodopa with different concentrations of BSA. [levodopa] = $3.00 \times 10^{-5}$ mol $L^{-1}$, [BSA] added at different concentrations, range = 0.00–$8.00 \times 10^{-6}$ mol $L^{-1}$ (in steps of $1.00 \times 10^{-6}$ mol $L^{-1}$).

### 3.2. Electrochemical behaviour of levodopa

Cyclic voltammograms of LD – an electrochemically active phenolic compound with two hydroxy and an amino group in its molecular structure, showed that LD has an oxidation peak at 330 mV (Fig. 2, curve 1) but only a very shallow reduction peak with its minimum at about 770 mV was observed; its better resolved wings appeared to be at about 230 mV (curve 1, Fig. 2). Since there was no evidence for a significant reduction process, it was concluded that the reaction at the electrode was irreversible. From the CV voltammogram (curve 1 in Fig. 2) of the LD at the glassy carbon electrode, the $E_p$ and $E_{p(1/2)}$ values were 330 and 275 mV, respectively. When irreversible oxidation occurs at an electrode, at $E_{p(1/2)}$, the corresponding current, $i$, is given by ($i_d/2$), and at 25 °C, $|E_p - E_{p(1/2)}| = 47.7/\alpha n$ [40], where $n$ is the electron transfer number, and $\alpha$ of an irreversible electrode process is generally assumed to be 0.5 [41]. Thus, $n$ was calculated to be 1.74 i.e. ~2. The oxidation reaction of LD at the surface of a glassy carbon electrode could then be described as in [42] (Illustrator 2).

BSA did not exhibit any observable peak at a glassy carbon electrode at pH 7.4; this pH was higher than the isoelectric point of BSA (pH 4.8) [43].

When BSA was added to the LD solution, the oxidation peak shifted towards higher potentials and a decreasing oxidation current was observed. This shift may be attributed to the changes of the molecular environment around the LD molecule as a result of its interaction with BSA [44]. This observation is consistent with the view that the LD–BSA interaction occurred between the most hydrophobic segment of the LD molecule [45] and the hydrophobic region of the BSA cavity.

### 3.3. Linear sweep voltammetry and fluorescence investigations of the LD–BSA system

The linear sweep voltammograms of LD/BSA mixtures in a Tris–HCl (pH 7.4) buffer solution collected at a glassy carbon electrode, indicated that the anodic peak current decreased continually and the peak potential shifted to more positive values with the addition of BSA (curves 1–19, Fig. 3A). The peak current from this LD reaction did not disappear completely with the increase of the BSA concentration; this is unexpected if a competitive adsorption occurred at the electrode. It has been observed, that when an interaction of some biopolymers such as hemoglobin, albumin and DNA with small molecules takes place at quite a low protein concentrations and a short accumulation time, only about 10% of the electrode surface may be covered; this implies that very little competitive adsorption of small molecules can occur [46]. The decrease in peak current without any changes in the electrochemical parameters suggested the formation of an electroinactive LD–BSA complex because LD becomes embedded within the BSA structure, which results in the decrease of the equilibrium concentration of LD in solution. However, there is another possible explanation for these observations, and it involves the possible unfolding of the BSA protein as the concentration of the ligand increases. As a result, the protein structure unravels, and this provides pathways for ligands to access the tryptophan or tyrosine residues, which then can be oxidized at the glassy carbon electrode (Scheme 1) [47].

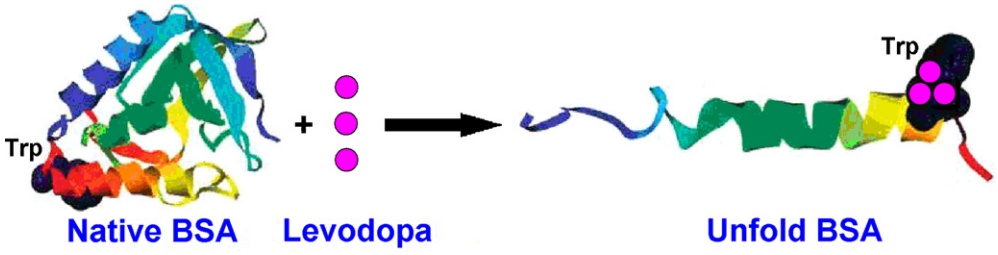


**Scheme 1.** Effect of the levodopa ligand on the tryptophan environment in protein.

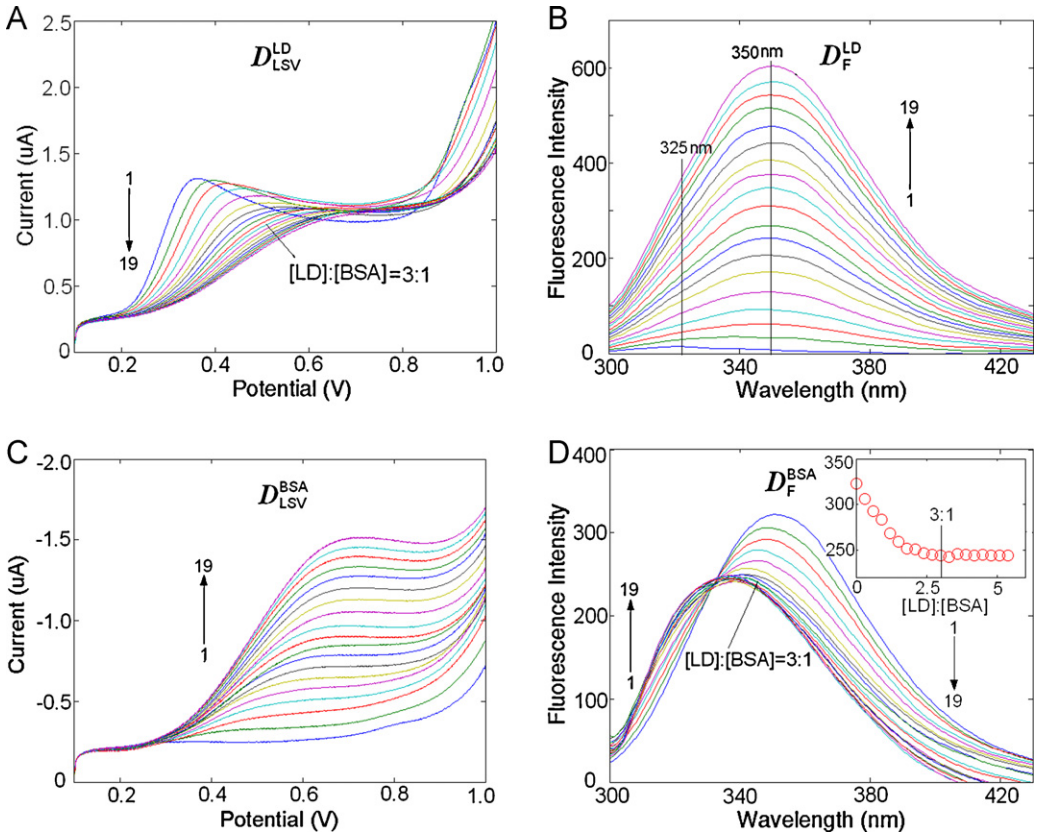


**Fig. 3.** Response profiles obtained from different experiments (Section 2.3.3) - experiments 1 and 2: (A) LSV ($\boldsymbol{D}^{LD}_{LSV}$) and (B) fluorescence ($\boldsymbol{D}^{LD}_{F}$); experiments 3 and 4: (C) LSV ($\boldsymbol{D}^{BSA}_{LSV}$) and (D) fluorescence ($\boldsymbol{D}^{BSA}_{F}$); inset figure – fluorescence intensity of BSA at 350 nm at different [LD]:[BSA] ratios.

When BSA was continually added to the LD, no change in peak current and peak potential was observed until a ratio of [LD]:[BSA] = 3:1 (curve 11; Fig. 3A). This indicated that the LD–BSA reaction approached equilibrium.

The fluorescence emission spectra of LD in the presence of BSA at various concentrations (Fig. 3B; experiment 2, Section 2.3.3) showed that with continuing addition of BSA, the emission peak of LD ($\lambda_{max}$ = 325 nm; curve 1) was effectively subsumed by subsequent spectra (curve 2 onwards); a new emission peak developed at 350 nm, which was assigned to BSA. The fluorescence intensity of this broad band increased proportionately, but no further information could be obtained from these overlapping spectra.

Typical linear sweep voltammograms of BSA ($1.00 \times 10^{-5}$ mol $L^{-1}$) in the presence of increasing concentrations of LD (Fig. 3C) supported the previous observations that BSA was electro-inactive at a glassy carbon electrode (curve 1) [48], but the peak current increased with the increase in concentration of the LD ligand (Fig. 3C). There was also a possible positive peak shift developing as well. With these observations, there was little strong evidence to suggest the formation of an LD–BSA complex, and consequently, it appeared that the increase in peak current was due mostly to the presence of free LD. Another possible explanation could be that the nature of the structural changes induced in BSA during its interaction with LD [47] resulted in the unfolding or denaturation of the protein; this facilitated easy access to the tryptophan and tyrosine residues for oxidation. The oxidation peak of the free LD and that of the tryptophan/tyrosine residues of LD–BSA complex overlap, and the recorded profile was the sum of these two phenomena, which increased together with the addition of LD.

Fluorescence of BSA originates from tryptophan, tyrosine and phenylalanine residues, where the source of the intrinsic fluorescence of BSA is mainly from the tryptophan residue alone. Emission fluorescence spectra of BSA in the presence of various concentrations of LD (Fig. 3D; experiment 4, Section 2.3.3) showed that the fluorescence intensity of BSA at 350 nm decreased steadily with the increasing concentration of the added LD ligand. However, at a ratio, $r_{LD:BSA}$, of about 3:1 (curve 11), this decrease effectively ceased, and a band peak at 335 nm became readily apparent; this was assigned to the free LD. In addition, an isoactinic point formed at 340 nm, which indicated an equilibrium between the free LD and the LD–BSA complex. The slight blue shift which became apparent could be ascribed to the effects of the intermolecular forces involved in maintaining the secondary structure of BSA; this could be slightly affected as a result of conformational changes in tryptophan and tyrosine micro-regions caused by interaction of LD with BSA.

Further discussion of the LD/BSA interaction on the basis of direct observations of the measured profiles was difficult because of band overlaps in the fluorescence spectra, and multivariate analysis previously discussed was applied to extract further information, especially as function of concentration of the LD and BSA reactants.

### 3.4. Fluorescence quantum yield for the system

The fluorescence quantum yield, $\Phi$, is a direct indication of the conversion efficiency of the absorbed photons into emitted photons. The $\Phi$, for the ligand, levodopa, and the complex, $(levodopa)_3$–BSA, were determined with the use of the reference, quinine sulfate ($\Phi$ = 0.546 in 1.0 mol $L^{-1}$ sulfuric acid) [49]; calculations of the $\Phi$ values are well established [50], and they were found to be 0.059 and 0.064 for levodopa, and $(levodopa)_3$–BSA, respectively. The fluorescence quantum yield of BSA at maximum excitation wavelength 280 nm was measured to be 0.130 [51]. The

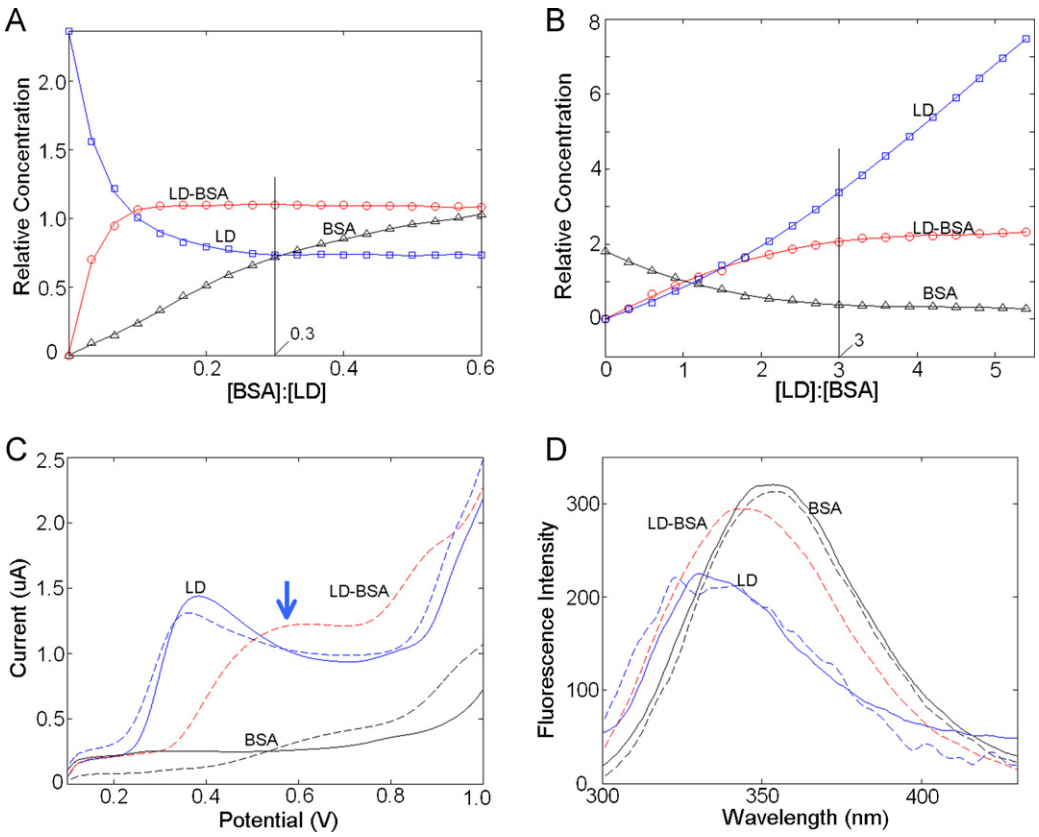


**Fig. 4.** Application of MCR–ALS: (A) and (B) Extracted concentration profiles; (C) and (D) measured (full curves) and extracted (dashed curves) voltammograms and fluorescence spectra of different species in the levodopa-BSA systems, obtained from the four experiments 1–4 (Section 2.3.3).

difference between the values of $\Phi$ (BSA) and $\Phi$ ((levodopa)$_3$–BSA) may be explained by the collisional quenching, which occurs when the BSA (excited state) in solution is deactivated on contact with levodopa.

### 3.5. Interpretation of the MCR–ALS results

As previously discussed in detail (Section 2.4), the fluorescence and the voltammetric profile matrices were combined into an expanded data matrix, $\begin{bmatrix} \boldsymbol{D}_{\mathrm{LSV}}^{\mathrm{LD}} & \boldsymbol{D}_{F}^{\mathrm{LD}} \\ \boldsymbol{D}_{\mathrm{LSV}}^{\mathrm{BSA}} & \boldsymbol{D}_{F}^{\mathrm{BSA}} \end{bmatrix}$, which was submitted for simultaneous resolution by the MCR–ALS method. The intention was to extract information regarding: (i) any drug–BSA complex, (ii) the relative concentrations of the various reacting species, and (iii) any effects of the ligands on the protein's sub-structure. Thus, after the construction of the expanded data matrix, the number of factors, i.e. the chemical species, was estimated with the use of the EFA procedure. EFA was basically designed to work with full rank two-way data sets and straightforward analysis of rank-deficient matrix does not provide useful information. To overcome this limitation, De Juan et al. [52] have recently proposed an evolution of the original algorithm. This new approach is based on a two-step strategy. First, rotational ambiguity is eliminated by matrix augmentation. The augmented data matrix, $\begin{bmatrix} \boldsymbol{D}_{\mathrm{LSV}}^{\mathrm{LD}} & \boldsymbol{D}_{F}^{\mathrm{LD}} \\ \boldsymbol{D}_{\mathrm{LSV}}^{\mathrm{BSA}} & \boldsymbol{D}_{F}^{\mathrm{BSA}} \end{bmatrix}$, is formed by column-wise and row-wise augmented data set. Then, EFA is applied to the unfolded full rank augmented data set eventually providing information about contributions that are otherwise hidden. PCA was also employed to select the appropriate number of components to describe the two systems, and it was found that the first three PCs explained 99.9% of the total data variance in the combined matrix $\begin{bmatrix} \boldsymbol{D}_{\mathrm{LSV}}^{\mathrm{LD}} & \boldsymbol{D}_{F}^{\mathrm{LD}} \\ \boldsymbol{D}_{\mathrm{LSV}}^{\mathrm{BSA}} & \boldsymbol{D}_{F}^{\mathrm{BSA}} \end{bmatrix}$ [53]. Thus, both the EFA and PCA methods estimate the same number of factors or chemical species involved, namely, the free BSA, free LD and ligand–BSA complex [29]. Also, the required initial estimates of the concentration profiles for these three postulated species were obtained from the EFA results, and were used to start the MCR–ALS data processing. The concentration calculations were optimized with modeling constraints: (i) the results were to be positive or zero, and (ii) only unimodal profiles were to be extracted. Also, as the total concentrations of LD and BSA were known in the experiments, they were included as closure constraints for the concentration profiles. The closure constraint is applied to closed reaction systems, where the principle of mass balance is fulfilled. With this constraint, the sum of the concentrations or fractions of all of the species involved in the reaction or mixture (the suitable elements in the $C$ matrix) is forced to be equal to a constant value (the total concentration or fractions) at each stage in the reaction or in the mixture. The lack of fit [54], which is defined as the difference between the input data, $D$, and the data reproduced from the $CS^{\mathrm{T}}$ product obtained by MCR–ALS, was used as a parameter to evaluate the goodness of fit of the model according to the following expression:

$$\text{lack of fit}\,(\%) = 100\sqrt{\frac{\sum_{i,j} e_{ij}^2}{\sum_{i,j} d_{ij}^2}} \tag{4}$$

where $d_{ij}$ is an element in the raw data and $e_{ij}$ is the corresponding residual after the model variation is removed. In this work, the lack of fit value was found to be 7.43%. This, in quantitative terms, implies that almost all of the variability in the experimental data, presented as a product of the extracted spectra and the

concentration profiles, is explained. However, this fit parameter provides an overall measure of the residual.

The experiments were based on the mole - ratio model and the concentration profiles ($\boldsymbol{C}^{LD}$ and $\boldsymbol{C}^{BSA}$) were extracted by the MCR–ALS method (Fig. 4A and B; experiments 1–2 in Section 2.3.3), respectively. They showed that: (i) with the mole–ratio method, the concentration of the LD–BSA intercalation complex increased sharply and reached equilibrium when the ratio, $r_{BSA:LD} \sim 0.3$ (Fig. 4A); (ii) the concentration of the intercalation complex increased slowly to $r_{LD:BSA} \sim 3$, and approached the equilibrium position as the concentration of LD increased (Fig. 4B). Thus, these results indicated that at equilibrium a 3:1 LD–BSA, i.e. $LD_3$–BSA complex forms.

The pure voltammetric and spectral profiles extracted by the application of the MCR–ALS method provided new qualitative information about the nature of the complex. The measured (full curves) and extracted (dashed curves) pure spectral and voltammetric profiles of LD agreed reasonably well (Fig. 4C and D; blue full and dashed curves); likewise, the fluorescence spectra of BSA were in good agreement. The extracted fluorescence spectrum (Fig. 4D dashed red line) of the LD–BSA complex was obtained for the first time, and was the first such spectral representation of the LD–BSA complex. Not surprisingly, its peak maximum fell between the LD and BSA bands at $\lambda = 346$ nm. The unique application of this band has already been demonstrated in the discussions of Fig. 4A and B above.

The extraction of the voltammetric profiles and their reasonable agreement with the measured data indicated that the MCR–ALS method was applied successfully (Fig. 4C). The BSA measured curve suggested that the protein in its original structural format was electroinactive, and the extracted profile approximated this profile–no obvious extracted bands were evident. However, the LD–BSA curve, unlike that for the BSA, indicated the presence of electroactive species; it had a peak potential maximum at about 0.58 V (see the arrow in Fig. 4C). To achieve this result for the reaction occurring at the electrode's surface, it is necessary for the potentially oxidizable tryptophan and tyrosine side chain residues to be accessible. This would be facilitated somewhat by an unfolded rather than the originally folded structure of the BSA protein. This has been previously discussed (Section 3.4), but with the original measurements, it was impossible to decide exactly what was happening. Now given the nature of the LD–BSA extracted voltammogram (Fig. 4C), it seemed reasonable to suggest that the binding of the three LD molecules facilitated the unfolding of the BSA structure (Scheme 1). It has been suggested that such an unfolding process can be used as a marker for conformational changes in this protein [47].

## 4. Conclusion

An analytical method was researched and developed for the detailed, simultaneous determination of reactants and products during the binding of important small molecules such as LD (or dopamine) with biopolymers such as BSA. Voltammetric and fluorescence spectroscopy methodology produced measured profiles from different reactant mixtures as a function of concentration. These results enabled the extraction of the equilibrium constants, $K_{SV}$, at different temperatures, which are reported for the first time; voltammetric results supported the formation of the LD–BSA complex but not that with dopamine, which suggested that this drug would be difficult to transport in a biological environment. Deeper interpretation of the LD–BSA system was precluded because the measured composite profiles could not be resolved.

New information resulted, when the extended data matrix was resolved by the MCR–ALS method. The extracted concentration profiles indicated that the drug:BSA stoichiometry was 3:1, i.e. $LD_3$–BSA. Significantly, the novel, extracted voltammogram profile of the LD–BSA complex showed that the complex was electroactive, which was unexpected if the LD ligand was embedded in the natural folded state of the BSA protein. Consequently, it is suggested that the protein with the three LD ligands was unfolded at the electrode.

This analytical approach could be just as revealing with similar complex reaction systems and is recommended for such applications.

## Acknowledgements

The authors gratefully acknowledge the financial support of this study by the National Natural Science Foundation of China (NSFC-21065007) and the State Key Laboratory of Food Science and Technology of Nanchang University (SKLF-TS-200919 and SKLF-KF-201004).

## References

[1] A.D. Juan, S.C. Rutan, R. Tauler, D.L. Massart, Chemom. Intell. Lab. Syst. 40 (1998) 19–32.
[2] M. Vives, R. Gargallo, R. Tauler, Anal. Chim. Acta 424 (2000) 105–114.
[3] Y.N. Ni, Y.H. Lai, S. Brandes, S. Kokot, Anal. Chim. Acta 647 (2009) 149–158.
[4] H.V. Barnes, Clinical Medicine, Year Book Medical Publisher, New York, 1988, pp. 745–750.
[5] M.F. Bergamini, A.L. Santos, N.R. Stradiotto, M.V.B. Zanoni, J. Pharm. Biomed. Anal. 39 (2005) 54–59.
[6] S.S. More, R. Vince, J. Med. Chem. 51 (2008) 4581–4588.
[7] W.M. Pardridge, Mol. Interv. 3 (2003) 90–105.
[8] U. Kragh-Hansen, Pharmacol. Rev. 33 (1981) 17–53.
[9] A. Sulkowska, J. Rownicka, B. Bojko, W. Sulkowski, J. Mol. Struct. 651 (2003) 133–140.
[10] R.K. Ockner, R.A. Weisiger, J.L. Gollan, Am. J. Physiol. Gastrointest. Liver Physiol. 245 (1983) G13–G18.
[11] Y.Y. Yue, X.G. Chen, J. Qin, X.J. Yao, J. Pharm. Biomed. Anal. 49 (2009) 753–759.
[12] J.S. Mandeville, E. Froehlich, H.A. Tajmir-Riahi, J. Pharm. Biomed. Anal. 49 (2009) 468–474.
[13] H.X. Luo, Y. Du, Z.X. Guo, Bioelectrochemistry 74 (2009) 232–235.
[14] Q.H. Lu, C.D. Ba, D.Y. Chen, J. Pharm. Biomed. Anal. 47 (2008) 888–891.
[15] C. Bertucci, V. Andrisano, R. Gotti, V. Cavrini, J. Chromatogr. B 768 (2002) 147–155.
[16] B. Bojko, A. Sulkowska, M. Maciazek-Jurczyk, J. Rownicka, W.W. Sulkowski, J. Mol. Struct. 924–926 (2009) 332–337.
[17] Y.N. Ni, S.S. Wang, S. Kokot, Anal. Chim. Acta 663 (2010) 139–146.
[18] Y.N. Ni, G.L. Liu, S. Kokot, Talanta 76 (2008) 513–521.
[19] R. Gusmao, C. Arino, J.M. Diaz-Cruz, M. Esteban, Analyst 135 (2010) 86–95.
[20] E. Chekmeneva, R. Prohens, J.M. Diaz-Cruz, C. Arino, M. Esteban, Environ. Sci. Technol. 42 (2008) 2860–2866.
[21] Y.N. Ni, S. Kokot, Anal. Chim. Acta 626 (2008) 130–146.
[22] A.C. Olivieri, Anal. Chem. 80 (2008) 5713–5720.
[23] L.A. MacManus-Spencer, M.L. Tse, P.C. Hebert, H.N. Bischel, R.G. Luthy, Anal. Chem. 82 (2010) 974–981.
[24] L. Fotouhi, S. Banafsheh, M.M. Heravi, Bioelectrochemistry 77 (2009) 26–30.
[25] T. Peter, All About Albumin: Biochemistry Genetics and Medical Applications, Academic Press, San Diego, CA, 1996, pp. 9–75.
[26] J. Jaumot, R. Gargallo, A. de Juan, R. Tauler, Chemom. Intell. Lab. Syst. 76 (2005) 101–110.
[27] H. Gampp, M. Maeder, C.J. Meyer, A.D. Zuberbühler, Talanta 32 (1985) 1133–1139.
[28] H. Abdollahi, V. Mahdavi, Langmuir 23 (2007) 2362–2368.
[29] S. Perez, M.J. Culzoni, G.G. Siano, M.D. Gil Garcia, H.C. Goicoechea, M.M. Galera, Anal. Chem. 81 (2009) 8335–8346.
[30] M. Vives, R. Gargallo, R. Tauler, Anal. Chem. 71 (1999) 4328–4337.
[31] A. Alberich, C. Arino, J.M. Diaz-Cruz, M. Esteban, Anal. Chim. Acta 584 (2007) 403–409.
[32] D.M. Charbonneau, H.A. Tajmir-RIAHI, J. Phys. Chem. B 114 (2010) 1148–1155.
[33] C.Q. Jiang, M.X. Gao, X.Z. Meng, Spectrochim. Acta A 59 (2003) 1605–1610.
[34] G.W. Zhang, Q.M. Que, J.H. Pan, J.B. Guo, J. Mol. Struct. 881 (2008) 132–138.
[35] J.R. Lakowicz, Principles of Fluorescence Spectroscopy, 2nd ed., Plenum Press, New York, 1999, 237 pp.
[36] F.M. Benes, Trends Pharmacol. Sci. 22 (2001) 46–47.
[37] Y.J. Hu, Y. Liu, J.B. Wang, X.H. Xiao, S.S. Qu, J. Pharm. Biomed. Anal. 36 (2004) 915–919.
[38] M.M. Patel, B.R. Goyal, S.V. Bhadada, J.S. Bhatt, A.F. Amin, CNS Drugs 23 (2009) 35–58.
[39] H.P. Wang, J.S. Lee, M.C. Tasi, H.H. Lu, W.L. Hsu, Bioorg. Med. Chem. Lett. 5 (1995) 2195–2198.
[40] A.J. Bard, L.R. Faulkner, Electrochemical Methods: Fundamentals and Applications, 2nd ed., Wiley, New York, 2001, 236 pp.
[41] E. Laviron, J. Electroanal. Chem. 52 (1974) 355–393.

[42] M. Aslanoglu, A. Kutluay, S. Goktas, S. Karabulut, J. Chem. Sci. 121 (2009) 209–215.
[43] Y.H. Wu, X.B. Ji, S.S. Hu, Bioelectrochemistry 64 (2004) 91–97.
[44] Y.N. Ni, X. Zhang, S. Kokot, Spectrochim. Acta A 71 (2009) 1865–1872.
[45] Z.W. Zhu, C. Li, N.Q. Li, Microchem. J. 71 (2002) 57–63.
[46] S.S. Kalanur, U. Katrahalli, J. Seetharamappa, J. Electroanal. Chem. 636 (2009) 93–100.
[47] B. Ojiha, G. Das, J. Phys. Chem. B 114 (2010) 3979–3986.
[48] L.H. Guo, N. Qu, Anal. Chem. 78 (2006) 6275–6278.
[49] J. Olmsted, J. Phys. Chem. 83 (1979) 2581–2584.
[50] M. Grabolle, M. Spieles, V. Lesnyak, N. Gaponik, A. Eychmüller, U. Resch-Genger, Anal. Chem. 81 (2009) 6285–6294.
[51] Y.P. Zhang, Y.J. Wei, N. Li, S.J. Qin, Chin. J. Anal. Chem. 32 (2004) 779–782.
[52] A. De Juan, S. Navea, J. Diework, R. Tauler, Chemom. Intell. Lab. Syst. 70 (2004) 11–21.
[53] A. Dominguez-Vidal, M.P. Saena-Navajas, M.J. Ayora-Canada, B. Lendl, Anal. Chem. 78 (2006) 3257–3264.
[54] C.B. Zachariassen, J. Larsen, F. Van den Berg, R. Bro, A. De Juan, R. Tauler, Chemom. Intell. Lab. Syst. 83 (2006) 13–25.